Radiology

ORIGINAL RESEARCH • THORACIC IMAGING

Abdominal Imaging Findings in COVID-19: Preliminary Observations

Rajesh Bhayana, MD, FRCPC • Avik Som, MD, PhD • Matthew D. Li, MD • Denston E. Carey, BSc • Mark A. Anderson, MD • Michael A. Blake, MD • Onofrio Catalano, MD • Michael S. Gee, MD, PhD • Peter F. Hahn, MD, PhD • Mukesh Harisinghani, MD • Aoife Kilcoyne, MBBCh, BAO • Susanna I. Lee, MD, PhD • Amirkasra Mojtahed, MD • Pari V. Pandharipande, MD, MPH • Theodore T. Pierce, MD • David A. Rosman, MD, MBA • Sanjay Saini, MD • Anthony E. Samir, MD, MPH • Joseph F. Simeone, MD • Debra A. Gervais, MD • George Velmahos, MD, PhD • Joseph Misdraji, MD • Avinash Kambadakone, MD, FRCR

From the Division of Abdominal Imaging, Department of Radiology (R.B., A.S., M.D.L., M.A.A., M.A.B., O.C., M.S.G., P.F.H., M.H., A. Kilcoyne, S.I.L., A.M., P.V.P., T.T.P., D.A.R., S.S., A.E.S., J.F.S., D.A.G., A. Kambadakone), Division of Trauma, Emergency Surgery, and Surgical Critical Care, Department of Surgery (G.V.), and Department of Pathology (J.M.), Massachusetts General Hospital, 55 Fruit St, Boston, MA 02114-2696; and Harvard Medical School, Boston, Mass (D.E.C.). Received April 29, 2020; revision requested May 4; revision received May 6; accepted May 11. **Address correspondence to** R.B. (e-mail: *rajesh.bhayana@uhn.ca*).

Conflicts of interest are listed at the end of this article.

Radiology 2020; 297:E207–E215 • https://doi.org/10.1148/radiol.2020201908 • Content codes: CH GI

Background: Angiotensin-converting enzyme 2, a target of severe acute respiratory syndrome coronavirus 2 (SARS-CoV-2), demonstrates its highest surface expression in the lung, small bowel, and vasculature, suggesting abdominal viscera may be susceptible to injury.

Purpose: To report abdominal imaging findings in patients with coronavirus disease 2019.

Materials and Methods: In this retrospective cross-sectional study, patients consecutively admitted to a single quaternary care center from March 27 to April 10, 2020, who tested positive for SARS-CoV-2 were included. Abdominal imaging studies performed in these patients were reviewed, and salient findings were recorded. Medical records were reviewed for clinical data. Univariable analysis and logistic regression were performed.

Results: A total of 412 patients (average age, 57 years; range, 18 to >90 years; 241 men, 171 women) were evaluated. A total of 224 abdominal imaging studies were performed (radiography, $n = 137$; US, $n = 44$; CT, $n = 42$; MRI, $n = 1$) in 134 patients (33%). Abdominal imaging was associated with age (odds ratio [OR], 1.03 per year of increase; $P = .001$) and intensive care unit (ICU) admission (OR, 17.3; $P < .001$). Bowel-wall abnormalities were seen on 31% of CT images (13 of 42) and were associated with ICU admission (OR, 15.5; $P = .01$). Bowel findings included pneumatosis or portal venous gas, seen on 20% of CT images obtained in patients in the ICU (four of 20). Surgical correlation ($n = 4$) revealed unusual yellow discoloration of the bowel ($n = 3$) and bowel infarction ($n = 2$). Pathologic findings revealed ischemic enteritis with patchy necrosis and fibrin thrombi in arterioles ($n = 2$). Right upper quadrant US examinations were mostly performed because of liver laboratory findings (87%, 32 of 37), and 54% (20 of 37) revealed a dilated sludge-filled gallbladder, suggestive of bile stasis. Patients with a cholecystostomy tube placed ($n = 4$) had negative bacterial cultures.

Conclusion: Bowel abnormalities and gallbladder bile stasis were common findings on abdominal images of patients with coronavirus disease 2019. Patients who underwent laparotomy often had ischemia, possibly due to small-vessel thrombosis.

The coronavirus disease 2019 (COVID-19) pandemic, caused by the severe acute respiratory syndrome coronavirus 2 (SARS-CoV-2), presents an ongoing global threat. Common clinical features reported in early confirmed infections included fever, cough, and myalgias or fatigue (1,2). As testing capacity and case numbers have increased worldwide, however, gastrointestinal (GI) symptoms, such as diarrhea, nausea, vomiting, abdominal pain, and loss of appetite, have been increasingly recognized (3–5). Although lung injury is most common, liver injury of uncertain origin has been observed in patients with COVID-19, with increased frequency in severe cases (6).

SARS-CoV-2 is thought to gain access to cells via surface expression of angiotensin-converting enzyme 2 (ACE2) (7). Thus, tissues with high levels of ACE2 expression are assumed to be susceptible to direct infection (8). ACE2 surface expression is most abundant in lung alveolar epithelial cells, enterocytes of the small intestine, and the vascular endothelium (9). The large amount of ACE2 surface expression in the GI tract and, to a lesser extent, in the biliary epithelium has been offered as a possible explanation for GI symptoms and liver injury (10,11). In addition, SARS-CoV-2 has been identified in stool samples of a substantial proportion of infected patients (12–14).

Several reports have evaluated chest imaging findings in patients with COVID-19, leading to a greater understanding of pathogenesis in the lung (15,16). Despite the widening recognition of abdominal manifestations, to our knowledge, corresponding abdominal imaging findings have not yet been reported. Imaging findings may increase the understanding of abdominal phenomena in SARS-CoV-2 infection. Further, radiologists should be aware of abdominal imaging findings in patients with COVID-19. The purpose of this study

Abbreviations

ACE2 = angiotensin-converting enzyme 2, COVID-19 = coronavirus disease 2019, GI = gastrointestinal, ICU = intensive care unit, OR = odds ratio, SARS-CoV-2 = severe acute respiratory syndrome coronavirus 2

Summary

Bowel abnormalities, including ischemia, were common findings on abdominal images of patients with coronavirus disease 2019.

Key Results

- Of inpatients with coronavirus disease 2019, 33% underwent abdominal imaging and 17% underwent cross-sectional imaging; imaging was associated with age (odds ratio [OR], 1.03 per year of increase) and intensive care unit (ICU) admission (OR, 17.3).
- Right upper quadrant US revealed findings of gallbladder bile stasis in 54% of examinations.
- Bowel-wall abnormalities were seen on 31% of CT images (3.2% of all patients); signs of late ischemia were seen on 20% of CT images in patients in the ICU (2.7% of patients in the ICU), with pathologic correlation suggesting small-vessel thrombosis.

is to explore abdominal imaging findings in patients with COVID-19.

Materials and Methods

Patients and Study Design

This was a retrospective cross-sectional study performed at a large quaternary care academic institution, with institutional review board approval and waiver of the requirement for informed consent. All data were collected in compliance with the Health Information Portability and Accountability Act. All aspects of the study were performed in accordance with the Declaration of Helsinki.

We included all adult patients (>18 years) who were consecutively admitted to our institution over a 2-week period (March 27 to April 10, 2020) and who tested positive for SARS-CoV-2. No patients were excluded. We queried our electronic radiologic database on our picture archiving and communications system to identify all abdominal imaging examinations performed in these patients from 7 days prior to admission to April 21, 2020. The patients underwent abdominal imaging studies, including radiography, US, CT of the abdomen and pelvis, and MRI.

Image Acquisition

All CT scans were performed on 64- or 128-slice multidetector CT scanners. The CT scans were performed with (n = 35) or without (n = 7) intravenous contrast media. In patients undergoing contrast material–enhanced CT, axial acquisition of abdominal and pelvic images in the portal venous phase was performed after injection of 80–120 mL of iodinated contrast media (350 mg of iodine per milliliter, Omnipaque; GE Healthcare, Marlborough, Mass) at a flow rate of 3–5 mL/sec followed by a 40-mL saline chaser at the same rate. Axial images were reconstructed at 5-mm thickness with an interval of 5 mm. Coronal and sagittal reformatted images were created at a 3-mm thickness. All US examinations were performed by a registered sonographer (1–30 years of experience).

Our limited right upper quadrant US protocol includes evaluation of the liver, gallbladder, central biliary tree, and portal vein. Cine and static gray-scale and color Doppler US images were acquired and sent to our picture archiving and communications system for interpretation by a fellowship-trained abdominal radiologist (1–47 years of experience). Radiographs were obtained with patients in the supine position, with scan coverage extending from above the dome of the diaphragm to below the pubic symphysis. The abdominal MRI examination (n = 1) was a gadolinium-enhanced liver 3-T MRI study.

Data Collection and Image Analysis

All cross-sectional imaging studies (US, CT, MRI) were interpreted in a clinical setting by a fellowship-trained abdominal radiologist (1–47 years of experience). Images were independently reviewed an average of 13 days after the initial report by a board-certified radiologist (R.B., an abdominal imaging fellow with 5 years of experience, including training), who was blinded to clinical data. Discrepancies regarding the initial interpretation were resolved via consensus in consultation with a fellowship-trained abdominal radiologist (A.K., 8 years of experience). Because assessment of certain features can be subjective, the following criteria were adhered to when reviewing images: *(a)* bowel-wall thickening on CT images was defined as single-wall thickness greater than 3 mm in distended loops and greater than 5 mm in collapsed loops; *(b)* fluid-filled colon was defined homogeneous, low-attenuation colonic content; *(c)* gallbladder distention was defined as a transverse dimension greater than 4 cm; *(d)* gallbladder sludge was defined as echogenic nonshadowing debris in the gallbladder; *(e)* gallbladder wall thickening was defined as single-wall thickness greater than 3 mm in an adequately distended gallbladder on US images specifically interrogating the gallbladder; and *(f)* fatty liver on US images was defined as increased echogenicity of the hepatic parenchyma obscuring periportal echogenicity with or without diaphragmatic echogenicity. These thresholds were intentionally set to be more specific than sensitive to reduce false-positive observations.

After review of imaging studies, surgical and pathologic notes were collected from electronic medical records and were reviewed by two radiologists (R.B., A.K.). Surgical findings were verified in consultation with a critical care surgeon (G.V., 26 years of experience). Pathology findings were verified by a GI pathologist, who reviewed pathologic images (J.M., 20 years of experience). Demographic and clinical data (presence of GI symptoms, intensive care unit [ICU] admission) were collected from electronic medical records by independent investigators (A.S., 1st-year radiology resident; M.D.L., 3rd-year radiology resident; or D.E.C., 3rd-year medical student), who were blinded to imaging findings. The presence of GI symptoms at admission was defined as documentation of nausea, vomiting, diarrhea, or abdominal pain on the clinical note at initial hospital evaluation. All data were compiled and analyzed by two radiologists (R.B., A.K.).

Statistical Analysis

Demographic, clinical, and imaging data from patients admitted to the ICU were compared with those of other inpatients using univariable statistical tests, including independent *t* tests, χ^2 tests, and Fisher exact tests. Logistic regression analyses were performed to assess for an association between imaging parameters (number of abdominal imaging studies, cholestasis, bowel wall abnormality) and demographic or clinical data (age, sex, GI symptoms at admission, ICU admission). *P* values less than .05 indicated a significant difference. All statistical analyses were performed using the stats package in *R* (version 3.6.3; R Foundation for Statistical Computing, Vienna, Austria) (17).

Results

Patient Characteristics and Imaging Use

A total of 412 adult patients who tested positive for SARS-CoV-2 were admitted to our institution during the study period, and of these, 136 (33%) were admitted to the ICU. Patients included 241 men (58%) and 171 women (42%), with an average age of 57 years ± 18 (range, 18 to >90 years). Patients admitted to the ICU were, on average, older than other inpatients (59 years vs 56 years, *P* = .04). The proportion of patients who initially presented with at least one GI symptom was 34% (*n* = 142 of 412), with no difference in the proportion between those admitted to the ICU and other inpatients (29% vs 37%, *P* = .08). Patients were followed for an average of 16.8 days (range, 11–25 days) after admission.

For all patients, 224 abdominal imaging studies were performed (radiography, *n* = 137; US, *n* = 44; CT, *n* = 42; MRI, *n* = 1) in 134 of 412 patients (33%). In total, 72 patients (17%) had at least one cross-sectional abdominal imaging study. Of patients who underwent cross-sectional imaging, 92% (*n* = 66 of 72) were admitted for a diagnosis of COVID-19, rather than for other reasons, and then had a positive test for SARS-CoV-2. Abdominal imaging studies were associated with age (odds ratio [OR], 1.03 per year of increase; *P* = .001) and ICU admission (OR, 17.3; *P* < .001). Abdominal imaging tended to be more likely in patients with GI symptoms at admission; however, this was not statistically significant (OR, 1.61, *P* = .09).

The most common indications for CT were abdominal pain (14 of 42, 33%) and sepsis (12 of 42, 29%). Of the US examinations performed (*n* = 44), right upper quadrant US was most common (*n* = 37 of 44; 84%). Most right upper quadrant US examinations were performed in patients admitted to the ICU (32 of 37, 86%). The most common indication for right upper quadrant US was abnormal liver laboratory findings (*n* = 31 of 37, 84%). Table 1 shows descriptive data of inpatients, including abdominal imaging studies performed and study indications.

CT Findings

Most CT scans were performed with intravenous contrast material (35 of 42, 83%). Bowel wall abnormalities were found on 31% (13 of 42) of abdominal CT images and were associated with ICU admission (OR, 15.5; *P* = .01). The presence of bowel wall abnormalities was not associated with age (OR, 1.06 per year of increase; *P* = .10), sex (female OR, 0.59; *P* = .54), or GI symptoms at admission (OR, 2.02; *P* = .40). Bowel wall thickening was identified on 29% (12 of 42) of CT images and included colon or rectal thickening (*n* = 7) and small-bowel thickening (*n* = 5) (Fig 1). Small-bowel thickening was exclusively seen in patients in the ICU in our study sample (ICU, *n* = 5; non-ICU, *n* = 0). Pneumatosis or portal venous gas (Figs 2–5) was identified on 20% of CT images obtained in patients in the ICU (four of 20), constituting 2.9% of all patients admitted to the ICU (four of 136). A vascular cause was not identified on any of these CT images. One of these patients (Fig 5) had pneumatosis cystoides intestinalis. In three of four patients with pneumatosis or portal venous gas, the finding was first identified on a radiograph (*n* = 2) or US image (*n* = 1) prior to CT being performed. One of the four patients had a perforated small bowel, as evidenced by frank bowel wall discontinuity (Fig 2a).

In one patient who underwent abdominal CT for GI symptoms, who was not being considered for SARS-CoV-2 infection at the time, lung base findings led to a diagnosis of COVID-19. Other CT findings included fluid-filled colon on 43% of images (18 of 42), suggestive of diarrhea. Patients in the ICU were more likely to have this finding than were other inpatients (65% vs 23%, *P* = .04). Two patients (4.8% of CT findings), both in the ICU, had evidence of at least one acute infarction in a solid organ (renal, splenic, or hepatic). CT findings are compiled in Table 2.

US Findings

Gallbladder sludge and distention were seen in 54% (20 of 37) of right upper quadrant US studies, suggestive of bile stasis (Fig 6). Findings of gallbladder bile stasis were not associated with age (OR, 1.03 per year of increase; *P* = .32), sex (female OR, 0.44; *P* = .36), ICU admission (OR, 5.83; *P* = .17), or GI symptoms at admission (OR, 1.97; *P* = .43). Four patients with findings of gallbladder bile stasis, all in the ICU, went on to have cholecystostomy tubes placed via interventional radiology that revealed negative bacterial cultures. US evidence of fatty liver was noted in 27% of studies (10 of 37). One patient in the ICU was incidentally found to have portal venous gas at US (Fig 4a), which was subsequently confirmed on CT images. US findings are outlined in Table 2.

Surgical and Pathologic Correlation

All patients with pneumatosis or portal venous gas at CT (*n* = 4), findings that were suggestive of ischemia, underwent exploratory laparotomy. Two patients were found to have a frankly necrotic bowel at surgery (those shown in Figs 2 and 3). In both patients, a yellow discoloration of small-bowel loops was specifically noted by the surgeon at laparotomy (Fig 2b); this was in contrast to the usual purple or black color of a necrotic bowel. One underwent bowel resection, with pathologic findings (Fig 3c) demonstrating ischemic enteritis with patchy necrosis ranging from mucosal necrosis to full-thickness necrosis. Subjacent to necrotic mucosa, submucosal arterioles contained fibrin thrombi, and others showed damage with perivascular neutrophils.

Table 1: Descriptive Data of Inpatients Who Tested Positive for SARS-CoV-2, Including Number of Abdominal Imaging Studies Performed and Study Indications

Parameter	All Inpatients	ICU	Non-ICU	*P* Value
No. of patients	412	136	276	
Age (y)*	57 (18 to >90)	59 (24 to >90)	56 (18 to >90)	.04
Sex				
Male	241 (58)	85 (63)	155 (56)	.26
Female	171 (42)	51 (38)	121 (44)	
GI symptoms at admission	142 (34)	40 (29)	102 (37)	.08
Patients with abdominal imaging†	134/224 (33)	97/178 (71)	37/46 (13)	<.001
Radiographs	79/137 (19)	69/125 (51)	10/12 (3.6)	<.001
All cross-sectional	72/87 (17)	43/53 (32)	29/34 (11)	<.001
All CT	40/42 (10)	20/20 (15)	20/22 (7.2)	.03
CT with contrast material	34/35 (8.3)	16/16 (12)	18/19 (6.5)	.14
All US	40/44 (10)	30/33 (22)	10/11 (3.6)	<.001
Right-upper-quadrant US	34/37 (8.3)	29/32 (21)	5/5 (1.8)	<.001
Renal US	5/6 (1.2)	0/0 (0)	5/6 (1.8)	.27
Testicular US	1/1 (0.2)	1/1 (0.7)	0/0 (0)	.72
MRI	1 (0.2); 1	0 (0); 0	1 (0.4); 1	>.99
Study indications				
Abdominal CT				
Pain	14 (33)	5 (25)	9 (41)	.34
Infectious source	12 (29)	8 (40)	4 (18)	.17
Nausea or vomiting	3 (7.1)	0 (0)	3 (14)	.23
Diarrhea	2 (4.8)	0 (0)	2 (9.1)	.49
GI bleed	2 (4.8)	2 (10)	0 (0)	.22
Ischemia	2 (4.8)	2 (10)	0 (0)	.22
Abnormal previously	2 (4.8)	2 (10)	0 (0)	.22
Other	5 (12)	1 (5)	4 (18)	…
Right upper quadrant US				
Elevated LFTs	32 (86)	27 (84)	5 (100)	>.99
Infectious source	3 (8.2)	3 (9.4)	0 (0)	>.99
Pain	2 (5.4)	2 (6.3)	0 (0)	>.99
Renal US				
AKI	3 (50)	0 (0)	3 (50)	…
Infectious source	3 (50)	0 (0)	3 (50)	…

Note.—Unless otherwise indicated, data are numbers of patients, with percentages in parentheses. $P < .05$ indicates a significant difference. AKI = acute kidney injury, GI = gastrointestinal, ICU = intensive care unit, LFT = liver function test, SARS-CoV-2 = severe acute respiratory syndrome coronavirus 2.

* Data are mean age, with the range in parentheses.

† Data are number of patients who underwent the imaging examination and total number of examinations performed in these patients, respectively, with the percentage of patients in parentheses.

The other two patients did not have frank bowel necrosis at laparotomy. In one, with ileal pneumatosis cystoides intestinalis at CT (Fig 5a, 5b), laparotomy demonstrated fibrotic ileum with pneumatosis but no obvious infarction. Pathology findings (Fig 5c, 5d) revealed diffuse ischemic injury with multifocal necrosis, marked submucosal edema with empty spaces consistent with pneumatosis (Fig 5c), and occasional fibrin thrombi in submucosal arterioles beneath necrotic mucosa (Fig 5d). In the last patient, who had mesenteric gas adjacent to the transverse colon (Fig 4b), patches of yellow discoloration on the antimesenteric aspect of the transverse colon were seen at surgery. Second-look laparotomic findings in this patient showed no infarcted bowel but did show yellow discoloration of the stomach. No bowel was resected in this patient.

Discussion

Abdominal manifestations, including gastrointestinal (GI) symptoms and liver enzyme elevation, have been reported frequently in patients with coronavirus disease 2019 (COVID-19) (1,3). However, to our knowledge, corresponding abdominal imaging findings have not been published. In our study, 34% of inpatients had GI symptoms at admission, which is similar to findings in recent reports (4,5). Abdominal imaging was

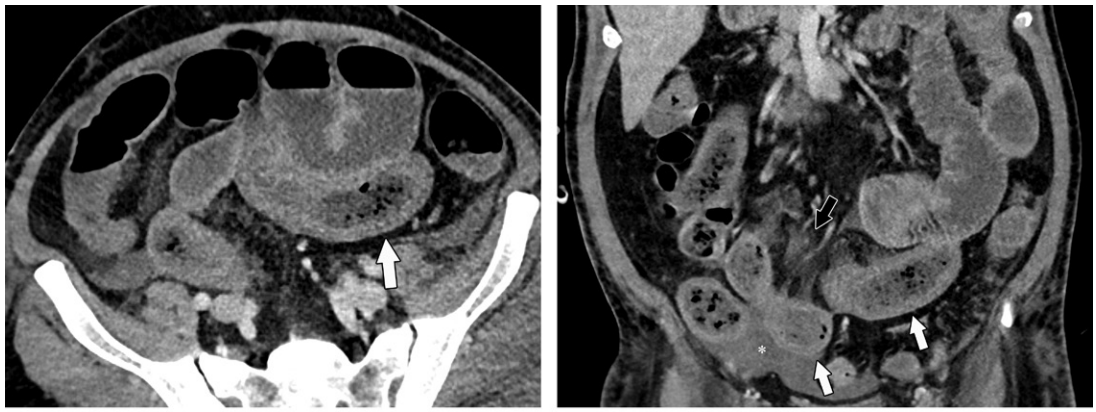

a. b.

Figure 1: **(a)** Axial and **(b)** coronal CT images of the abdomen and pelvis with intravenous contrast material in a 57-year-old man with high clinical suspicion for bowel ischemia. There is generalized small-bowel distension and segmental thickening (white arrows), with adjacent mesenteric congestion (black arrow) and a small volume of ascites (*). Findings are nonspecific but suggestive of early ischemia or infection.

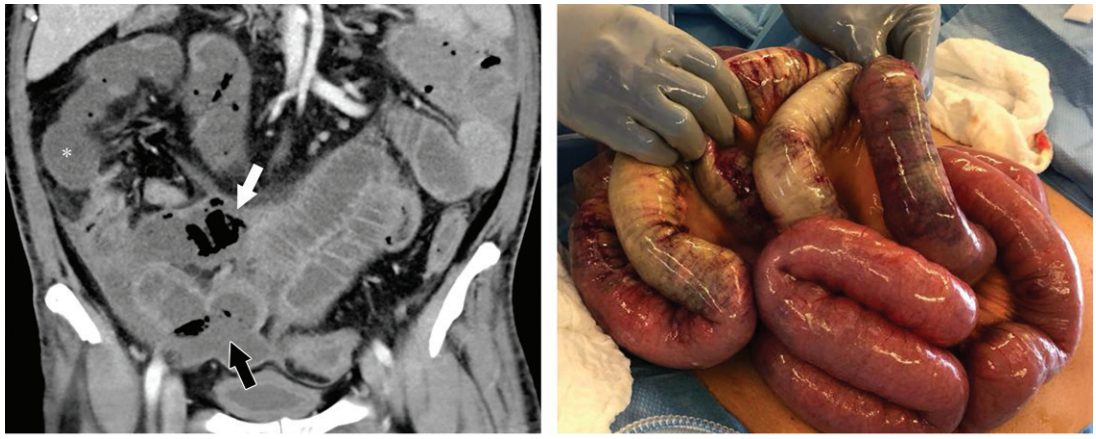

a. b.

Figure 2: **(a)** Coronal CT image of the abdomen and pelvis with intravenous contrast material in a 47-year-old man with abdominal tenderness shows typical findings of mesenteric ischemia and infarction, including pneumatosis intestinalis (white arrow) and nonenhancing bowel (*). Frank discontinuity of a thickened loop of small bowel in the pelvis (black arrow) is in keeping with perforation. **(b)** These findings are confirmed at laparotomy, with the additional observation of an atypical yellow discoloration of the bowel.

performed in 33% of inpatients with COVID-19, and 17% of patients had cross-sectional imaging. CT was most commonly performed for abdominal pain or sepsis, and US was most frequently performed for elevated liver enzyme levels.

Bowel wall findings were common on CT images and were associated with ICU admission (OR, 15.5; P = .01). Findings included bowel-wall thickening, pneumatosis, and portal venous gas. Pneumatosis and portal venous gas are often seen in patients with mesenteric ischemia, which is common in critically ill patients (18); however, numerous other causes, including viral enteritis and positive-pressure ventilation, exist (19,20). Of the four patients in our series with pneumatosis or portal venous gas, three had either frank bowel infarction at laparotomy (n = 2) or ischemic mucosal necrosis at pathologic examination (n = 2). At laparotomy, a yellow appearance of bowel was noted in three patients. Bowel infarction with gangrenous change can appear tan-yellow, which likely explains this appearance in the two patients with an infarcted bowel at surgery (21). However, one patient in our study with gas in the transverse mesocolon at CT (Fig 4b) had corresponding patchy yellow discoloration of the antimesenteric transverse colon of unknown origin.

Possible explanations for the spectrum of bowel findings in patients with COVID-19 include direct viral infection, small-vessel thrombosis, or nonocclusive mesenteric ischemia. ACE2 surface expression is most abundant in the lung alveolar epithelium, enterocytes of the small intestine, and vascular endothelium, suggesting that the small bowel and vasculature may be susceptible to SARS-CoV-2 infection (8,9). Findings suggestive of SARS-CoV-2 having a direct inflammatory effect on the vascular endothelium have been reported (22). Further, systemic coagulopathy is common in critically ill patients with COVID-19 (23). This observation has been supported by descriptions of complement-mediated microvascular injury and vascular imaging abnormalities (24,25). Pathology findings in patients with bowel resection in our series demonstrated ischemic mucosal necrosis and fibrin thrombi in

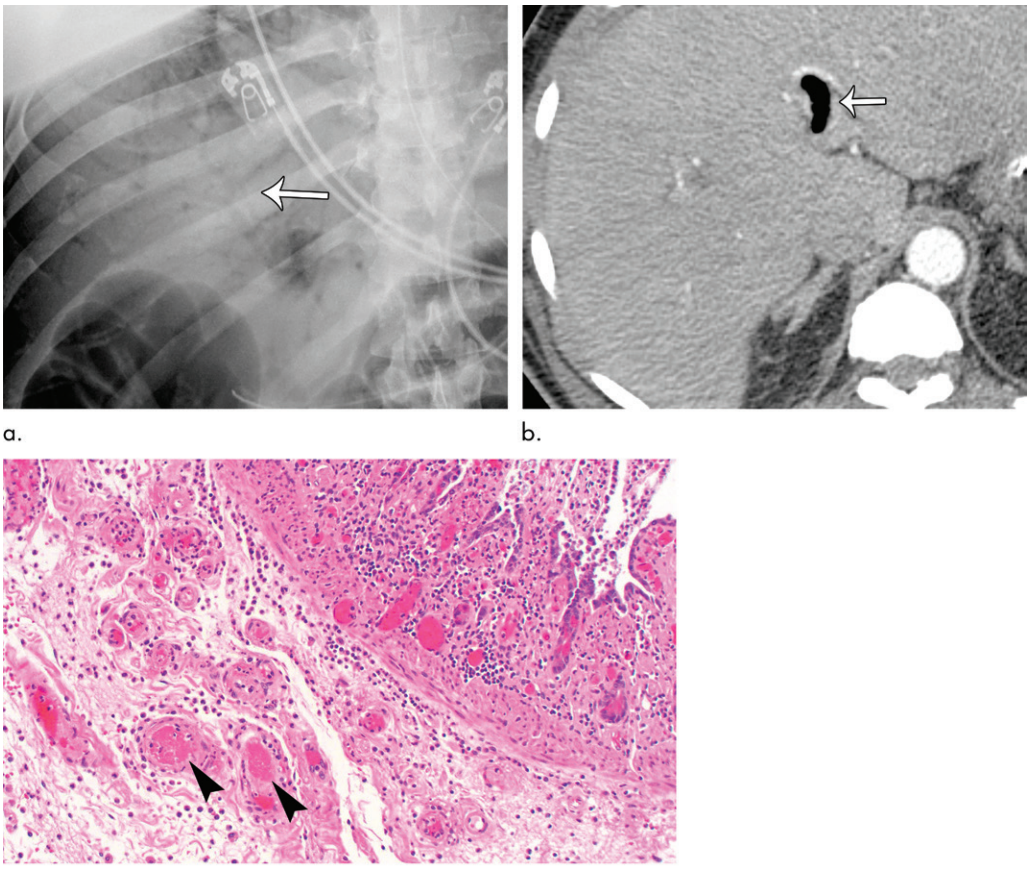

Figure 3: **(a)** Abdominal radiograph in a 52-year-old man show portal venous gas (arrow), suggestive of bowel infarction. **(b)** Postoperative CT image also shows portal venous gas (arrow). At laparotomy, bowel ischemia and necrosis are identified, along with an atypical yellow discoloration of the small bowel. **(c)** Photomicrograph shows submucosal arterioles with fibrin thrombi (arrowheads). The overlying mucosa (upper right) is partially necrotic, with crypt dropout and partial loss of the surface epithelium. (Hematoxylin-eosin stain; original magnification, ×400.)

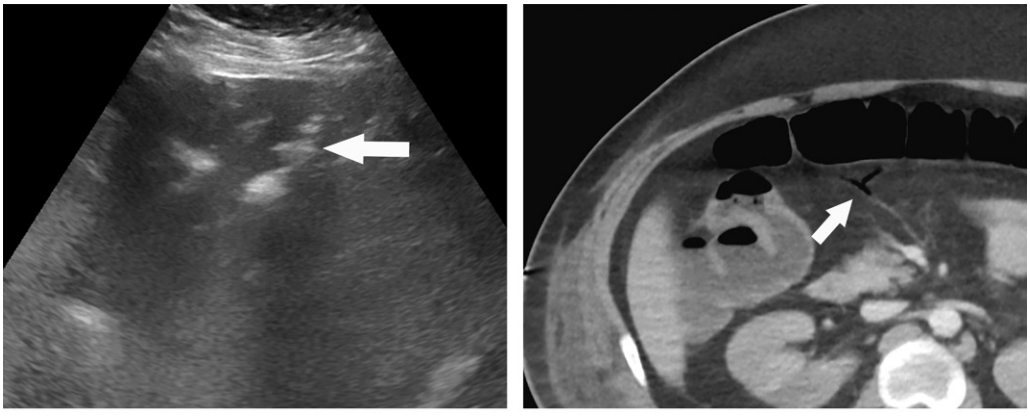

Figure 4: **(a)** Abdominal US obtained because of elevated liver enzyme level in a 34-year-old man incidentally shows peripheral echogenic branching foci (arrow) with dirty shadowing (*), in keeping with portal venous gas. **(b)** Subsequent CT image of the abdomen and pelvis with intravenous contrast material enabled confirmation of portal venous gas and shows gas in the transverse mesocolon vasculature (arrow). At laparotomy, patchy areas of yellow discoloration of uncertain origin are identified on the antimesenteric aspect of the transverse colon. Second-look laparotomy shows yellow discoloration of the stomach and no ischemia.

submucosal arterioles of necrotic segments. Although it can be difficult to determine whether fibrin thrombi are the cause of ischemia in bowel necrosis, given the coagulopathy these patients experience, they are likely pathogenic (26). The biologic basis that explains the spectrum of bowel imaging findings in patients with COVID-19 warrants further investigation.

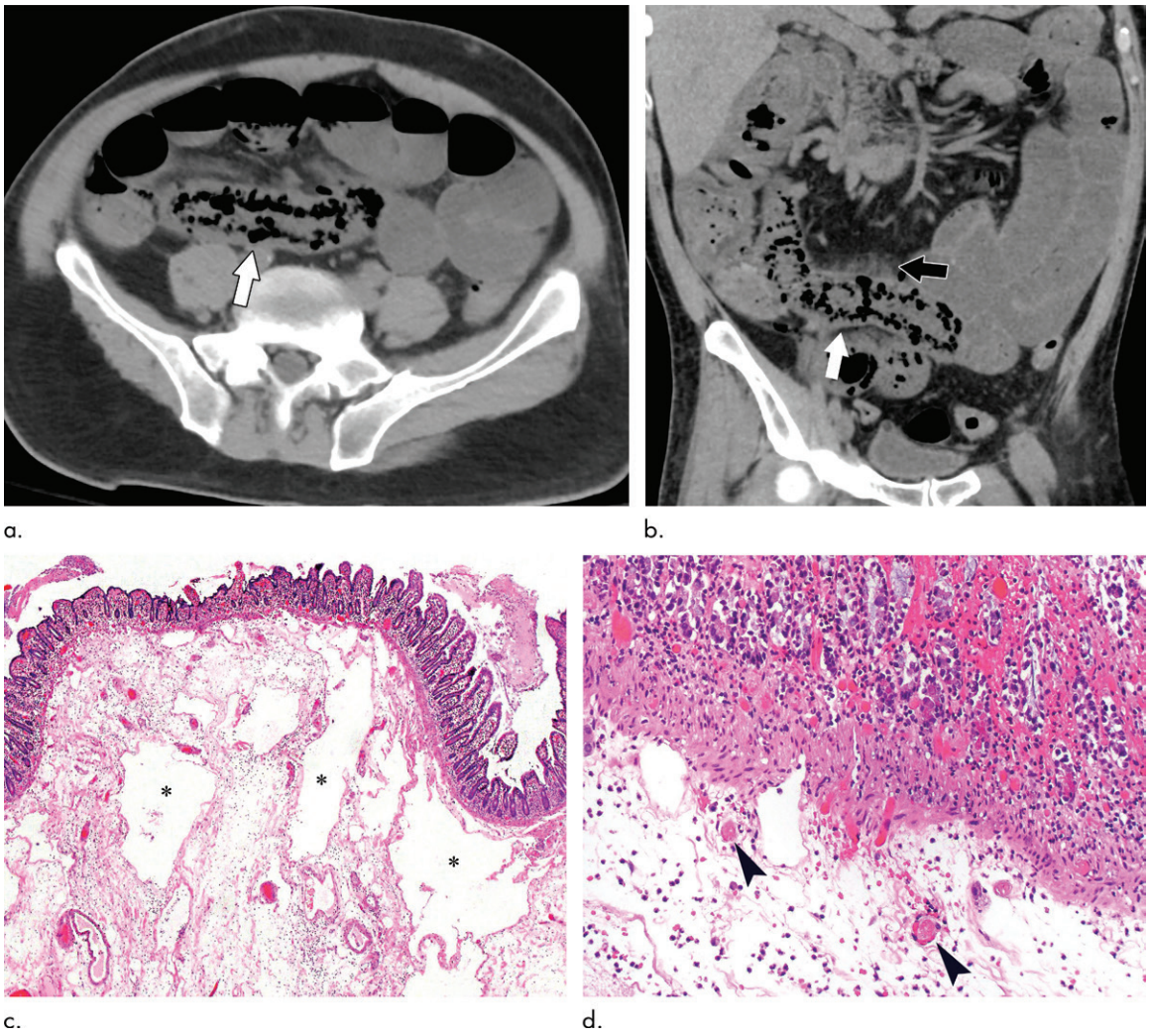

Figure 5: Nonenhanced **(a)** axial and **(b)** coronal CT performed in a 54-year-old man shows pneumatosis cystoides intestinalis (white arrows) in a long segment of ileum. Adjacent mesenteric congestion is also noted (black arrow). Laparotomy shows no frank bowel necrosis. **(c)** A low-power photomicrograph of the ileum shows ischemic degenerative changes of the mucosa, with villous blunting (left) and withered crypts. There is marked submucosal edema with large empty spaces, consistent with pneumatosis (*). (Hematoxylin-eosin stain; original magnification, ×40.) **(d)** A high-power view of the superficial submucosa shows arterioles with fibrin thrombi (arrowheads) beneath the damaged mucosa. (Hematoxylin-eosin stain; original magnification, ×40.)

In three of the four patients with pneumatosis or portal venous gas, the finding was initially identified on radiographic or US studies. This emphasizes the importance of radiologists being alert to findings obtained with all imaging modalities. Although US is sensitive for portal venous gas, radiography is insensitive for both pneumatosis and portal venous gas (27). Two cases of pneumatosis or portal venous gas in our series were initially detected with radiography, the most commonly performed modality in our study, raising the possibility that these manifestations are present more frequently than we have recognized. On CT images, a fluid-filled colon was seen frequently, often considered to indicate diarrhea. Diarrhea is common in patients in the ICU (28), and fluid-filled colon was more common in these patients in our study. However, GI symptoms such as diarrhea are common at admission in patients with COVID-19 and can be overlooked (3). Although liquid stool often escapes comment on CT images, this finding might provide the first indication of GI symptoms in patients with COVID-19.

Although elevated liver enzyme levels have been reported frequently in patients with COVID-19 (1,6), the cause is uncertain. Findings of gallbladder bile stasis were seen on 54% of right upper quadrant US images in our series. Of the 20 patients with findings of cholestasis, four had cholecystostomy tubes placed that had negative bacterial cultures. Imaging and laboratory findings of cholestasis are common in critically ill patients admitted to the ICU (29,30). Although patients with COVID-19 in the ICU are often hypercoagulable (31), we did not identify any patients with portal vein thrombosis.

The main limitation of this study was that it was a single-center retrospective study, which limits its generalizability and introduces selection bias. Pathologic correlation and clinical follow-up was not available for many patients with imaging abnormalities.

In conclusion, abdominal imaging was often performed for inpatients with coronavirus disease 2019 (COVID-19). Right upper quadrant US most frequently demonstrated gallbladder

Table 2: CT and Right Upper Quadrant US Imaging Findings in Inpatients Who Tested Positive for SARS-CoV-2

Imaging Findings	All Patients	Patients in the ICU	Patients Not in the ICU	*P* Value
CT of abdomen and pelvis	42	20	22	
Abnormal bowel wall	13 (31)	10 (50)	3 (14)	.02
Colonic or rectal thickening	7 (17)	4 (20)	3 (14)	.69
Small-bowel thickening	5 (12)	5 (25)	0 (0)	.02
Pneumatosis or PV gas	4 (9.5)	4 (20)	0 (0)	.04
Perforation	1 (2.4)	1 (5)	0 (0)	.48
Fluid-filled colon, *n* (%)	18 (43)	13 (65)	5 (23)	.01
Solid organ infarction	2 (4.8)	2 (10)	0 (0)	.22
Pancreatitis	1 (2.4)	0 (0)	1 (4.5)	>.99
Findings suggestive of hepatitis (GB thickening, heterogeneous liver)	1 (2.4)	1 (5)	0 (0)	.48
Right-upper-quadrant US	37	32	5	
GB sludge and distension	20 (54)	19 (59)	1 (20)	.16
GB sludge, nondistended	2 (5.4)	2 (6.3)	0 (0)	>.99
GB wall-thickening	1 (2.7)	1 (3.1)	0 (0)	>.99
Pericholecystic fluid	1 (2.7)	1 (3.1)	0 (0)	>.99
Fatty liver	10 (27)	8 (25)	2 (40)	0.6
PV gas	1 (2.7)	1 (3.1)	0 (0)	>.99
Portal vein thrombosis	0 (0)	0 (0)	0 (0)	…

Note.—Data are numbers of patients, with percentages in parentheses. $P < .05$ indicates a significant difference. GB = gallbladder, ICU = intensive care unit, PV = portal venous, SARS-CoV-2 = severe acute respiratory syndrome coronavirus 2.

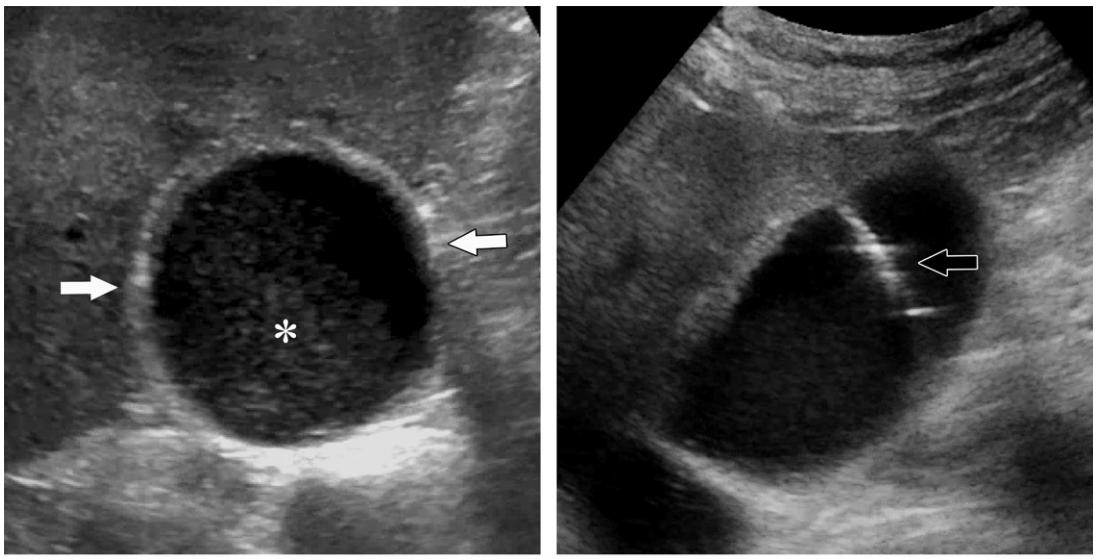

Figure 6: **(a)** Abdominal US image of an 83-year-old man with an elevated liver enzyme level and sepsis shows a distended gallbladder (arrows) containing sludge (*), suggestive of cholestasis. **(b)** Intraprocedural US image shows a needle within the gallbladder lumen (arrow), while a cholecystostomy tube is placed with US guidance. Fluid analysis reveals noninfected bile.

bile stasis, which is common in critically ill patients. Bowel wall abnormalities identified with CT, mostly in patients in the ICU, included pneumatosis and portal venous gas suggestive of ischemia. Laparotomic and pathologic findings enabled us to confirm small-bowel ischemia in some patients, which may have been due to small-vessel thrombosis. The cause of bowel abnormalities in patients who did not undergo surgery remains uncertain. Further studies are required to clarify the cause of bowel findings in patients with COVID-19, in particular the role of small-vessel thrombi and coagulopathy in bowel ischemia, and to determine whether severe acute respiratory syndrome coronavirus 2 plays a direct role in bowel or vascular injury.

Acknowledgments: The authors thank Nick Reid, BSc, Nicholos Joseph, BA, J. C. Panagides, BEng, Tristan Yeung, BSc, Min Lang, MD, Brent Little, MD, Efren Flores, MD, and Dexter Mendoza, MD, of the Harvard Medical School Coronavirus Disease radiology research group for aid in data collection and institutional review board approval.

Author contributions: Guarantors of integrity of entire study, R.B., A.E.S., A. Kambadakone; study concepts/study design or data acquisition or data analysis/interpretation, all authors; manuscript drafting or manuscript revision for important intellectual content, all authors; approval of final version of submitted manuscript, all authors; agrees to ensure any questions related to the work are appropriately resolved, all authors; literature research, R.B., A.S., D.E.C., M.A.B., O.C., M.H., A. Kilcoyne, A.M., D.A.R., A.E.S.; clinical studies, R.B., A.S., M.D.L., D.E.C., M.A.A., M.A.B., O.C., P.F.H., M.H., A. Kilcoyne, S.I.L., A.M., S.S., J.F.S., A. Kambadakone; experimental studies, O.C.; statistical analysis, R.B., O.C.; and manuscript editing, R.B., A.S., D.E.C., M.A.A., M.A.B., O.C., M.S.G., P.F.H., A. Kilcoyne, S.I.L., A.M., P.V.P., T.T.P., D.A.R., S.S., D.A.G., G.V., A. Kambadakone.

Disclosures of Conflicts of Interest: R.B. disclosed no relevant relationships. **A.S.** disclosed no relevant relationships. **M.D.L.** disclosed no relevant relationships. **D.E.C.** disclosed no relevant relationships. **M.A.A.** disclosed no relevant relationships. **M.A.B.** disclosed no relevant relationships. **O.C.** disclosed no relevant relationships. **M.S.G.** Activities related to the present article: disclosed no relevant relationships. Activities not related to the present article: received research funding from Takeda-Millennium Pharmaceuticals. Other relationships: disclosed no relevant relationships. **P.F.H.** disclosed no relevant relationships. **M.H.** disclosed no relevant relationships. **A. Kilcoyne** disclosed no relevant relationships. **S.I.L.** Activities related to the present article: disclosed no relevant relationships. Activities not related to the present article: received royalties from Wolters-Kluwer and Springer. Other relationships: disclosed no relevant relationships. **A.M.** disclosed no relevant relationships. **P.V.P.** disclosed no relevant relationships. **T.T.P.** disclosed no relevant relationships. **D.A.R.** disclosed no relevant relationships. **S.S.** disclosed no relevant relationships. **A.E.S.** disclosed no relevant relationships. **J.F.S.** disclosed no relevant relationships. **D.A.G.** disclosed no relevant relationships. **G.V.** disclosed no relevant relationships. **J.M.** disclosed no relevant relationships. **A. Kambadakone** Activities related to the present article: disclosed no relevant relationships. Activities not related to the present article: received grants from GE Healthcare and Philips. Other relationships: disclosed no relevant relationships.

References

1. Huang C, Wang Y, Li X, et al. Clinical features of patients infected with 2019 novel coronavirus in Wuhan, China. Lancet 2020;395(10223):497–506. [Published correction appears in Lancet 2020;395(10223):496.].
2. Guan WJ, Ni ZY, Hu Y, et al. Clinical characteristics of coronavirus disease 2019 in China. N Engl J Med 2020;382(18):1708–1720.
3. Luo S, Zhang X, Xu H. Don't overlook digestive symptoms in patients with 2019 novel coronavirus disease (COVID-19). Clin Gastroenterol Hepatol 2020;18(7):1636–1637.
4. Cholankeril G, Podboy A, Aivaliotis VI, et al. High prevalence of concurrent gastrointestinal manifestations in patients with SARS-CoV-2: early experience from California. Gastroenterology doi:10.1053/j.gastro.2020.04.008. Published online April 10, 2020. Accessed April 17, 2020.
5. Cheung KS, Hung IF, Chan PP, et al. Gastrointestinal manifestations of SARS-CoV-2 infection and virus load in fecal samples from the Hong Kong cohort and systematic review and meta-analysis. Gastroenterology doi:10.1053/j.gastro.2020.03.065. Published online April 3, 2020. Accessed April 17, 2020.
6. Zhang C, Shi L, Wang FS. Liver injury in COVID-19: management and challenges. Lancet Gastroenterol Hepatol 2020;5(5):428–430.
7. Hoffmann M, Kleine-Weber H, Schroeder S, et al. SARS-CoV-2 cell entry depends on ACE2 and TMPRSS2 and is blocked by a clinically proven protease inhibitor. Cell 2020;181(2):271–280.e8.
8. Zou X, Chen K, Zou J, Han P, Hao J, Han Z. Single-cell RNA-seq data analysis on the receptor ACE2 expression reveals the potential risk of different human organs vulnerable to 2019-nCoV infection. Front Med 2020;14(2):185–192.
9. Hamming I, Timens W, Bulthuis MLC, Lely AT, Navis G, van Goor H. Tissue distribution of ACE2 protein, the functional receptor for SARS coronavirus. A first step in understanding SARS pathogenesis. J Pathol 2004;203(2):631–637.
10. Xiao F, Tang M, Zheng X, Liu Y, Li X, Shan H. Evidence for gastrointestinal infection of SARS-CoV-2. Gastroenterology 2020;158(6):1831–1833.e3.
11. Chai X, Hu L, Zhang Y, et al. Specific ACE2 expression in cholangiocytes may cause liver damage after 2019-nCoV infection. bioRxiv 2020.02.03.931766v1 [preprint] https://www.biorxiv.org/content/10.1101/2020.02.03.931766v1. Posted February 4, 2020. Accessed April 17, 2020.
12. Han C, Duan C, Zhang S, et al. Digestive symptoms in COVID-19 patients with mild disease severity: clinical presentation, stool viral RNA testing, and outcomes. Am J Gastroenterol doi:10.14309/ajg.0000000000000664. Published online April 15, 2020. Accessed April 17, 2020.
13. Wang W, Xu Y, Gao R, et al. Detection of SARS-CoV-2 in different types of clinical specimens. JAMA doi:10.1001/jama.2020.3786. Published online March 11, 2020. Accessed April 17, 2020.
14. Wu Y, Guo C, Tang L, et al. Prolonged presence of SARS-CoV-2 viral RNA in faecal samples. Lancet Gastroenterol Hepatol 2020;5(5):434–435.
15. Bernheim A, Mei X, Huang M, et al. Chest CT findings in coronavirus disease-19 (covid-19): relationship to duration of infection. Radiology 2020;295(3):200463.
16. Song F, Shi N, Shan F, et al. Emerging 2019 novel coronavirus (2019-nCoV) pneumonia. Radiology 2020;295(1):210–217.
17. R: the R project for statistical computing. R Foundation Web site. https://www.R-project.org/. Accessed April 24, 2020.
18. Guillaume A, Pili-Floury S, Chocron S, et al. Acute mesenteric ischemia among postcardiac surgery patients presenting with multiple organ failure. Shock 2017;47(3):296–302.
19. Ho LM, Paulson EK, Thompson WM. Pneumatosis intestinalis in the adult: benign to life-threatening causes. AJR Am J Roentgenol 2007;188(6):1604–1613.
20. Pear BL. Pneumatosis intestinalis: a review. Radiology 1998;207(1):13–19.
21. Mitsudo S, Brandt LJ. Pathology of intestinal ischemia. Surg Clin North Am 1992;72(1):43–63.
22. Varga Z, Flammer AJ, Steiger P, et al. Endothelial cell infection and endotheliitis in COVID-19. Lancet 2020;395(10234):1417–1418.
23. Tang N, Li D, Wang X, Sun Z. Abnormal coagulation parameters are associated with poor prognosis in patients with novel coronavirus pneumonia. J Thromb Haemost 2020;18(4):844–847.
24. Caruso D, Zerunian M, Polici M, et al. Chest CT Features of COVID-19 in Rome, Italy. Radiology doi:10.1148/radiol.2020201237. Published online April 3, 2020. Accessed April 17, 2020.
25. Magro C, Mulvey JJ, Berlin D, et al. Complement associated microvascular injury and thrombosis in the pathogenesis of severe COVID-19 infection: a report of five cases. Transl Res doi:10.1016/j.trsl.2020.04.007. Published online April 15, 2020. Accessed April 17, 2020.
26. Brandt LJ, Gomery P, Mitsudo SM, Chandler P, Boley SJ. Disseminated intravascular coagulation in nonocclusive mesenteric ischemia: the lack of specificity of fibrin thrombi in intestinal infarction. Gastroenterology 1976;71(6):954–957.
27. Nelson AL, Millington TM, Sahani D, et al. Hepatic portal venous gas: the ABCs of management. Arch Surg 2009;144(6):575–581; discussion 581.
28. Tirlapur N, Puthucheary ZA, Cooper JA, et al. Diarrhoea in the critically ill is common, associated with poor outcome, and rarely due to *Clostridium difficile*. Sci Rep 2016;6(1):24691.
29. Molenat F, Boussuges A, Valantin V, Sainty JM. Gallbladder abnormalities in medical ICU patients: an ultrasonographic study. Intensive Care Med 1996;22(4):356–358.
30. Murray FE, Stinchcombe SJ, Hawkey CJ. Development of biliary sludge in patients on intensive care unit: results of a prospective ultrasonographic study. Gut 1992;33(8):1123–1125.
31. Spiezia L, Boscolo A, Poletto F, et al. COVID-19-related severe hypercoagulability in patients admitted to intensive care unit for acute respiratory failure. Thromb Haemost 2020. 10.1055/s-0040-1710018. Published online April 21, 2020..